RESEARCH PAPER

Monitoring the convection coefficient in fermentative processes using numerical methods

Priscila Marques da Paz[1] · Juliana de Oliveira[1]

Abstract

This work is based on the importance of monitoring the thermodynamic variables of sugarcane juice fermentation by *Saccharomyces cerevisiae*, using a numerical technique, and providing artifices that lead to the best performance of this bioprocess. Different combinations of yeast quantity were added to diverse dilutions of cane juice, allowing the evaluation of the fermentation performance. This was conducted by observing the temperature signal obtained from thermal probes inserted in the experimental set up. The best performances are utilized in the mathematical model evaluation. Thus, the signal reconstructed by the appropriate inverse problem and subsequently, regularized by the simplified method of least squares (the method used for adjusting the defined parameters) allows a common method to process the convection coefficient that can be monitored and controlled within an actuation range. This leads to an increased level of refinement in the technique. Results show that it is possible to determine the best parameters for this technique and observe the occurrence of fermentation by monitoring the temperature signal, thereby ensuring the realization of a high-quality and high-performance bioprocess.

Keywords Alcoholic fermentation · Convection coefficient · Inverse problem · Regularization · Temperature

Introduction

In recent years, there has been a considerable rise in the production of biofuels worldwide, especially ethanol and biodiesel [4]. The former, i.e., ethanol is the main purpose of this work, in the context of sugarcane fermentation. Because this is one of the most economical forms of alcohol production and the climatic and soil conditions in Brazil are suitable for sugarcane cultivation, this technique is extensively used there. In addition, due to the variability of factors that are used in its cultivation, sugarcane may contain a varied composition of water, sugars, fibers, and minerals. The juice obtained from its milling is suitably diluted to undergo the process of fermentation. Therefore, the microorganisms involved in the process have access to the fermentable sugars for feeding [1, 12].

One of the most commonly used microorganisms for alcoholic fermentation is *Saccharomyces cerevisiae*, which belongs to the group of mesophilic yeasts, i.e., yeasts capable of being active at room temperature. Because it is one the most widely studied eukaryotic organisms, whose metabolism is best understood, it has significant economic importance in biotechnological processes such as baking and ethanol production. The optimum temperature for the industrial production of ethanol is in the range of 299.15–308.18 K. However, the fermentative process being exothermic, the temperature can often reach 311.15 K. The rise in temperature, leads to an increase of the fermentation speed and favors bacterial contamination. At the same time, the yeast becomes more sensitive to ethanol toxicity. However, temperature rise leads to a greater loss of ethanol by evaporation in open fermentation tanks [12].

Another factor that raises the fermentation speed and, consequently, its productivity, is the increase in sugar concentration, which also causes an osmotic stress in the yeast [9, 11, 12, 19]. Additionally, the yeast concentration also influences the performance of the fermentation process, and at higher concentration, the process is faster and more

✉ Juliana de Oliveira
  juliana@assis.unesp.br

  Priscila Marques da Paz
  primpaz@gmail.com

1 Department of Biological Sciences, Faculty of Sciences and Letter of Assis (FCLA), University of São Paulo State (UNESP), Av. Dom Antônio 2100, Assis, São Paulo 19806-900, Brazil

productive. The yeast concentration controls the influence of the contaminating bacteria, thereby limiting its own growth. This becomes an important natural controller of the fermentative environment, by regulating the level of maintenance energy. Therefore, determining the ideal amount of both yeast and sugar and correlating these factors with the temperature of the fermentation process is necessary to obtain the best alcoholic fermentation [12]. This temperature describes the exothermic behavior of the chemical reactions that control the fermentation process, i.e., the amount of heat released from each glucose molecule when transformed into alcohol. This process takes place in the presence of heat previously received from the environment, and is necessary to initialize and maintain the vital functionality of the yeast. In this way, it is believed that monitoring and controlling the temperature during the fermentation process is fundamental to guarantee a high-quality and good performance of the process. Usually, fermentation control can be done by working with properties that govern it, such as extract concentration, temperature change during the process, and others [9]. An alternative to complement quality and safety of fermentation performance is to attenuate noises and delays from temperature signals acquired by thermal probes during this process, through numerical models. Thus, the process will be described with more real data, free from cited interferences [16].

The problematics involved in temperature signal control during alcoholic fermentation require the implementation of monitoring and control techniques, to guarantee high-quality and operational safety of systems in which the heat transfer phenomena (conduction, convection, and radiation) occur [16]. Heat transfer can be divided into direct and inverse processes. The first one involves the determination of temperature distribution of the medium, where all the relevant thermo-physical properties are known. The second aims at the same, but in the absence of data related to thermo-physical properties, which arise from the fermentation process. Inverse heat transfer problems are known to be ill-posed, i.e., at least one of the three conditions given by Hadamard, among the existence, uniqueness, and stability of the solution, is not satisfied. For instance, small variations in input data provoke considerable changes in the solution, indicating a lack of stability. Hence, although the method of inverse problem is more appropriate to obtain input data, the means to reconstruct the actual process temperature and its characteristic ill conditioning strongly amplify the neglected experimental errors, thereby completely corrupting the temperature reconstruction process [3, 5, 13, 14]. As experimental errors and distortions during temperature measurement are unavoidable, special techniques, such as regularization methods [20], need to be applied to contour such problems, for improving the reconstruction process, and ultimately, achieving acceptable results.

Regularization methods consist of modification of the ill-posed problem into a well-posed one, and the analysis of data from this new well-conditioned problem [3]. The simplified method of least squares (SMLS) was proposed for real-time [16] reconstruction of the original process temperature from a distorted, delayed, and noisy signal measured by an intrusive thermal probe. The problem formulation considers the processes of thermal accumulation, convection, and radiation. The probe time constant and the radiation coefficient depend on the convection coefficient.

Considering the importance of monitoring and controlling the performance of alcoholic fermentation, this work aims to determine the best fermentation performance by increasing the amount of heat release and duration of the process, by combining different amounts of yeast and water-diluted sugarcane juice for bioprocess evaluation. Once, the best performance of fermentation is defined, the temperature signal is applied on the numerical technique of regularization developed in this work [16] for obtaining the best parameters, necessary for the adjustment equation of this variable. Once both the equational data for better signal adjustments and the combinations necessary to obtain the best fermentation are maintained, the temperature data is re-collected from this type of fermentation, using two pairs of probes. As the convection process is approximately analogous in both the probes, the corresponding model can be used to generate a convection coefficient common to the process, refining the adjustment technique and providing appropriate range of performance for monitoring and controlling of the process temperature signal.

Materials and methods

As shown in the flowchart (Fig. 1), the whole process was developed in stages, mainly divided between alcoholic fermentation and numerical method. Each of these divisions describes, in a generic way, the flow of the stages that make up each one of the subjects, where arrows indicate the flow direction. The stages in which there were communications between these divisions, i.e., where the numerical method is applied to the data obtained by fermentation, are highlighted, and they directly correspond to the objectives of this work.
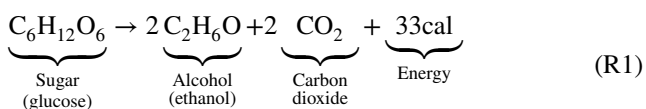
Fermentation

The fermentative process is further divided into substrate preparation, fermentation, and distillation. The first stage consists of milling the sugarcane, allowing the fermentable sugars to be extracted and exposed to the environment
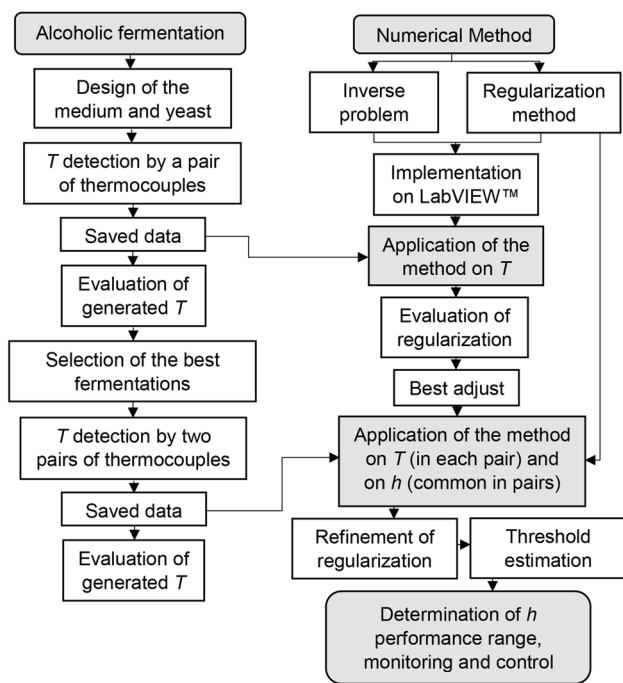
Fig. 1 Methodology flowchart. The steps of applying the numerical method in the fermentation are highlighted, T is temperature and h is the convection coefficient

containing microorganisms. This facilitates the occurrence of the second stage, which turns these sugars into ethanol and carbon dioxide. Besides the energy release corresponding to each consumed glucose molecule, there is an increase in the intrinsic temperature during the fermentation process, as shown in the stoichiometric and caloric reaction of alcoholic fermentation (R1). In the last stage, to separate the residues from the obtained ethanol, it is necessary to carry out the process of distillation [6, 11, 12]. Considering the objectives of this work, the third step need not be performed, because the proposed mathematical model uses the temperature data collected during the fermentation stage.

$$\underbrace{C_6H_{12}O_6}_{\substack{\text{Sugar}\\\text{(glucose)}}} \rightarrow 2\underbrace{C_2H_6O}_{\substack{\text{Alcohol}\\\text{(ethanol)}}} + 2\underbrace{CO_2}_{\substack{\text{Carbon}\\\text{dioxide}}} + \underbrace{33\text{cal}}_{\substack{\text{Energy}}} \qquad \text{(R1)}$$

Medium of culture

For carrying out fermentation, the biological agent *S. cerevisiae* was used in a granular and dry form of baking powder (Dona Benta Fermix, J. Macêdo, Fortaleza, Brazil). Different amounts of yeast M_Y (or mass of yeast, given in grams) were weighed using an analytical balance (AY220, Shimadzu, Kyoto, Japan), and tested on certain combinations of the fermentative medium.

Fermentative medium

The sugarcane used belongs to the genus *Saccharum* L., and was thoroughly cleaned with water and chopped to facilitate its milling, where the process is carried out with the aid of a commercial sugar mill. The juice obtained may have a varied composition of water, sugars, fibers, and minerals depending on the factors that characterize the sugarcane. Generally, the raw juice is composed of around 80% water, 10–20% sucrose, 0.1–2% reducing sugars, 0.3–0.5% ashes, and 0.5–1% nitrogenous compounds [12]. Conveniently, dilution of juice [D_J, given in percentage (%) of raw juice in distilled water] is linked with the alcoholic fermentation performance and, therefore, experiments were performed considering different D_J's. The juice was diluted with a graduated volumetric polypropylene test tube and placed in a 250 mL glass bottle with a lid. The same procedure was repeated for a second bottle that did not contain yeast, to obtain the fermentation control (standard).

Procedures for obtaining the best fermentation performance

The experiment was conducted according to a previously reported process [18], with some adaptations and scaled according to a lab set-up, using the Laboratory of Cellular and Molecular Immunology of UNESP of Assis for its design and execution. It involves the fermentation of a 150 mL of water-diluted juice, where D_J is equivalent to 10, 50, 66.7, and 100%—or pure broth, which usually corresponds to a range of 15–17 Brix [15]. Mass M_Y is equivalent to 1.0, 3.0, 5.4, and 10.0 g. When D_J and M_Y values are combined, 16 combinations of potentially high-performance fermentation processes are generated. Each set of experiment, F_n (fermentation number n, where $1 \le n \le 16$ with interval of 1) is formed by a pair of containers, filled with 150 mL of diluted juice. To one of them, yeast is added after insertion of the thermal sensors and proper care is taken, as will be described later. The other is used as the control (standard). The lids of both the containers are made of rubber thread, with a hole designed for the insertion of the thermocouples. The one in which fermentation takes place, an additional outlet for escape of CO_2 is provided, which is metallic, attached with a removable rubber hose, and has its other end placed in a beaker with distilled water. The containers' rims were sealed with a flexible film (Parafilm M®, Bemix, Neenah, USA) to avoid any contamination.

To initiate the process in the fermentation container, previously weighed yeast is inserted through the outlet of CO_2 with the aid of a funnel. The collection of temperature data for both the containers is performed using the data acquisition board (National Instruments, Austin, USA), rack type with USB CDAQ-9171 connection and

an analog output module for thermocouples (NI 9211) with four channels of 80 mV output, sampling rate 14 S/s and 24 bit resolution. For temperature measurement, type K thermocouples are used. The board is connected to the computer and measurements are displayed and saved by the acquisition system implemented in LabVIEW™ software (version 11.0, National Instruments, Austin, USA), with a built-in NI-DAQMX driver. The data collection is real-time and integral, i.e., it is neither paused nor aborted from the moment it is read in the container having yeast, till the end of the fermentation process.

The environment was maintained at room temperature, $T_{room} = 303.15$ K during the 24 h experiment, using a microprocessor controlled drying and heating chamber (Q317M-22, Quimis, Diadema, Brazil). Acquisition of temperature during these fermentation processes was conducted using a pair of thermocouples inserted inside the control, and another one in the container where fermentation takes place. One out of each thermocouple pair was encapsulated with silicon and all of them were connected to the acquisition board. Subsequently, their data was transferred and saved by the LabVIEW™ software. The temperatures acquired by the thermocouple pair inserted in the fermentation container will be denominated as the process temperature (actual, unprotected) and indicated temperature (encapsulated), denoted as $T_{proc,f}$ and $T_{ind,f}$, respectively. Similarly, the temperatures acquired by the thermocouple pair inserted inside the control will be read as $T_{proc,c}$ and $T_{ind,c}$, and may act as references to $T_{proc,f}$ and $T_{ind,f}$, respectively.

The data collected on $T_{proc,f}$, $T_{ind,f}$, $T_{proc,c}$, and $T_{ind,c}$ by the acquisition system were subsequently viewed in a table format in the Excel software (version 1611, Microsoft, Washington, USA). Next, the graph corresponding to the acquisition of the experiment F_n was obtained, by evaluating the maximum temperatures reached, i.e., $T_{proc,f}$ (max) and $T_{ind,f}$ (max), with their respective $T_{proc,c}$ and $T_{ind,c}$ along with the duration of fermentation, i.e., F_n. The differences between these temperatures can be presented as equations $\Delta T_{proc,f-c} = (T_{proc,f} \text{ (max)} - T_{proc,c})$, $\Delta T_{ind,f-c} = (T_{ind,f} \text{ (max)} - T_{ind,c})$, and the duration of fermentation Δt_f, measured in hours, is obtained by interpolating the time points' interval in which fermentation takes place.

In addition, these datasets were pre-treated for viewing in the numerical temperature adjustment system, whose equations were implemented in LabVIEW™ and are defined in "Mathematical formulation". The treatment consists of excluding the first points where the system has just received the yeast (when the fermentation has not yet started), and the last points (when the fermentation has ended).

Procedures to obtain the convection coefficient from the best fermentation performance

The experiment was carried out in a way similar to "Procedures for obtaining the best fermentation performance", but only for the best fermented output, as defined in "Evaluation of fermentation performance" of this work. The difference between the procedure of this item and the previous one, is that, here, four thermocouples were inserted in the same fermentation container, as indicated in Fig. 3, comprising of two pairs of thermocouples which allowed the generation of a common convection coefficient, using an appropriate mathematical model described in "Mathematical formulation".

The strategy of monitoring and controlling the convection coefficient considers the temperature measurement of a flow by two pairs of thermocouples having the same external geometry, but with different time constants, due to the different encapsulations of each pair.

At this stage, the thermocouples will be named as $T_{procA,f}$, $T_{indA,f}$, $T_{procB,f}$, and $T_{indB,f}$, respectively, representing the process and indicated temperatures of the pair A and B, and the ones indicated are the encapsulated thermocouples. Each thermocouple indicates a distorted and delayed T_{ind}, which can be reconstructed by the appropriate reverse regularized model, generating the reconstructed temperature T_{rec} by the inverse problem and the regularized temperature T_{reg} by SMLS.

Assuming, that the convection process is approximately same in both thermocouples, the corresponding model can be used to calculate a common convection coefficient, as shown in Fig. 2.

The data on $T_{procA,f}$, $T_{indA,f}$, $T_{procB,f}$, and $T_{indB,f}$ collected by the acquisition system was subjected to a treatment similar to the previously described technique in "Procedures for obtaining the best fermentation performance", and are destined to be read in the numerical adjustment system. This was implemented to receive the adjustments in the values of temperature and convection coefficient.

Mathematical formulation

Method of regularization

According to Ref. [16], Eq. (1) represents the transduction equation of the thermocouples, which relates the process temperature T_{proc} (K) and the indicated temperature T_{ind} (K), acquired by the thermocouple without and with the encapsulation at its end.

$$MC\frac{dT_{ind}}{dt} - hA(T_{proc} - T_{ind}) - \varepsilon\sigma A(T_{\infty}^4 - T_{ind}^4) = 0 \qquad (1)$$

This equation considers the thermal accumulation, characterized by the mass of the thermocouple tip M (kg) and
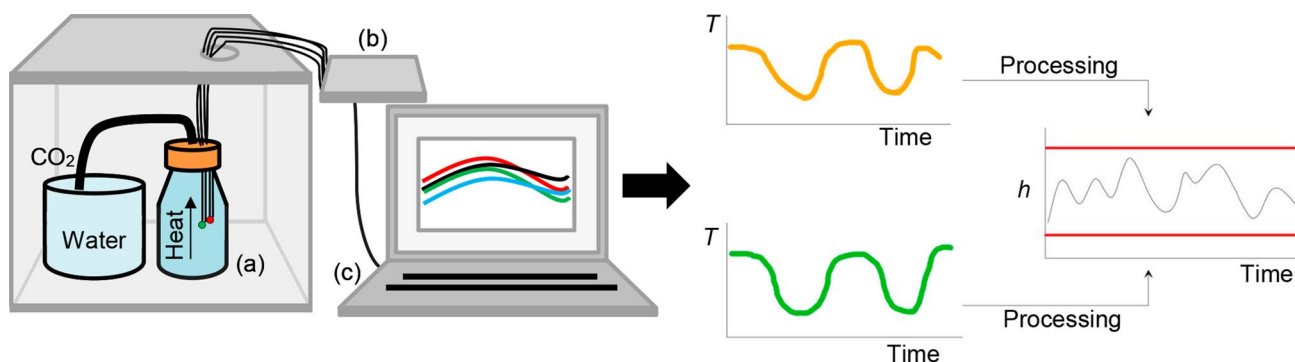
Fig. 2 Schematic diagram representing fermentation with the best performance using two pairs of thermocouples to generate temperature data to be applied in the numerical setting, resulting in the monitoring of convection coefficient, common to the process. Thermocouples are inserted into the fermentation container (**a**), connected to the acquisition board (**b**), and their data is transferred and saved by LabVIEW™ (**c**) for posteriorly processing

its specific heat capacity C (J/kg K). It also considers the amount of heat transferred by convection and radiation that is recorded at the sensor end through the thermocouple surface area A (m^2). The convection coefficient is h (W/m²K) and the surface emissivity is ε (dimensionless constant between 0 and 1), the Stefan–Boltzmann constant is $\sigma = 5.67 \times 10^{-8}$(W/m^2 K^4) and the free-stream temperature is denoted by T_∞ (K).

Equation (1) can be written in more appropriate terms, dividing both sides by hA and rearranging T_{ind} and T_∞, resulting in Eq. (2):

$$\tau \frac{dT_{ind}}{dt} - (T_{proc} - T_{ind}) - \gamma(T_\infty - T_{ind}) = 0, \tag{2}$$

where

$$\tau = \frac{MC}{hA}, \tag{3}$$

$$\gamma \cong \frac{4\varepsilon\sigma}{h}\left(\frac{T_\infty + T_{ind}}{2}\right)^3. \tag{4}$$

In Eq. (3), τ represents the thermocouple time constant (given in seconds), corresponding to the increase in temperature caused by the accumulated thermal and heat transfer by convection. The radiation coefficient γ from Eq. (4), in turn, quantifies the intensity of heat transferred by radiation.

Equation (2) expresses the relationship between the process variable (input) and the indicated one (output). Once the output variable T_{ind} is obtained by the encapsulated thermocouple, it is possible to determine the actual process temperature (input variable) using the inverse problem, as proposed in [16]. According to [16], the derivative of Eq. (2) acts as a high-pass filter and hence, the low-frequency elements of the T_{ind} signal are smoothed out, while the high frequency noise is amplified. In practice, this means that the

solutions resulting from the inverse problem usage will be strongly affected by the presence of experimental errors in T_{ind} measurements, generating T_{rec}. It is for this reason that the regularization method SMLS is applied, generating T_{reg}.

Dividing Eq. (1) by hA and considering two pairs of thermocouples A and B generates Eqs. (5) and (6):

$$\frac{M_A C_A}{hA}\frac{dT_{indA}}{dt} - (T_{proc} - T_{indA}) - \frac{\varepsilon\sigma}{h}(T_\infty{}^4 - T_{indA}{}^4) = 0, \tag{5}$$

$$\frac{M_B C_B}{hA}\frac{dT_{indB}}{dt} - (T_{proc} - T_{indB}) - \frac{\varepsilon\sigma}{h}(T_\infty{}^4 - T_{indB}{}^4) = 0. \tag{6}$$

Isolating and equating the expressions for T_{proc} from Eqs. (5) and (6), gives Eq. (7):

$$\frac{M_A C_A}{hA}\frac{dT_{indA}}{dt} + T_{indA} - \frac{\varepsilon\sigma}{h}(T_\infty{}^4 - T_{indA}{}^4)$$
$$= \frac{M_B C_B}{hA}\frac{dT_{indB}}{dt} + T_{indB} - \frac{\varepsilon\sigma}{h}(T_\infty{}^4 - T_{indB}{}^4). \tag{7}$$

The term $\frac{\varepsilon\sigma}{h}(T_\infty{}^4)$ is the same to both thermocouples and thus, gives Eq. (8):

$$\frac{M_A C_A}{hA}\frac{dT_{indA}}{dt} + T_{indA} + \frac{\varepsilon\sigma T_{indA}{}^4}{h}$$
$$= \frac{M_B C_B}{hA}\frac{dT_{indB}}{dt} + T_{indB} + \frac{\varepsilon\sigma T_{indB}{}^4}{h}, \tag{8}$$

which can be rearranged by isolating the indicated convection coefficient h_{ind} according to Eq. (9):

$$h_{ind} = \frac{1}{A(T_{indA} - T_{indB})}$$
$$\left[M_B C_B \frac{dT_{indB}}{dt} - M_A C_A \frac{dT_{indA}}{dt} + A\varepsilon\sigma\left(T_{indB}{}^4 - T_{indA}{}^4\right)\right]. \tag{9}$$

The regularization technique adopted by [16], which proved to be efficient for obtaining the process temperature in real-time, is applied to Eq. (9), for reasons similar to those for applying in T_{rec}, generating T_{reg}. This will be suitable for monitoring the convection coefficient.

The technique applied in [16] is known as the SMLS, whose basic idea is to fit a low-degree polynomial N for the last indicated temperatures for $m + 1$ (number of points) and replaces dT_{ind}/dt and T_{ind} in Eq. (9) by the smoothed or regularized values obtained from this polynomial.

Following the algorithm presented in [16], $T_{reg}(x) = a_0 + a_1 x + a_2 x^2 + \cdots + a_N x^N$ is the polynomial, where x is a support axis centered on the last acquired temperature and in an opposed form, oriented in time. The system formed by the polynomial must be solved by the SMLS to adjust the coefficients with the error minimization scheme, obtaining:

$$T_{ind}(n\Delta t) \cong T_{reg}(0) = a_0, \tag{10}$$

$$\frac{dT_{ind}}{dt}(n\Delta t) \cong -\frac{dT_{reg}}{dx}(0) = -a_1. \tag{11}$$

The values of Eqs. (10) and (11) are replaced in Eq. (9) and subsequently the regularized convection coefficient is obtained from smoothed values of T_{ind}, therefore, h_{reg} results in Eq. (12):

$$h_{reg} = \frac{1}{A\Delta t(a_{0A,n} - a_{0B,n})}$$
$$[M_A C_A a_{1A,n} - M_B C_B a_{1B,n} + A\varepsilon\sigma\left(a_{0B,n}^4 - a_{0A,n}^4\right)]. \tag{12}$$

The convection coefficient values are updated at each iteration n, and consequently, a graph is built for its monitoring.

However, in certain iterations, divisions by zero are performed in Eq. (12), which causes discontinuities in h_{reg} signal, as shown in [17]. This behavior is present even using simulated numerical values as input. To minimize this problem, apart from monitoring, a control system was developed so that the generated graph of h_{reg} is maintained within a predetermined range of operation.

Determination of the action range h

For this work, the method of control system implementation is similar to that performed in [17], but calculations to determine the action range of the graph are based on a threshold estimator (λ), as proposed in [7], and denominated as the Universal Threshold, in Eq. (13):

$$\lambda = \phi\sqrt{2\log\eta}, \tag{13}$$

where ϕ is an estimator of the standard deviation of noise and η is the sample size of h_{reg}. In a previously reported work

[10], it is suggested that the use of a robust estimator for ϕ, is based on wavelet coefficients at the finest level, according to Eq. (14):

$$\phi = \frac{\text{median}(h_{reg})}{0.6745}. \tag{14}$$

From the obtained value of λ, it is therefore possible to determine the control graph limits of h_{reg}, which are the tools of the statistical process control [2]. In this work, the central line that makes up the control graph is obtained by the median value of h_{reg} and corresponds to the stage of the process under control. Two parallel lines, above and below the central line, are plotted corresponding to the upper (UL) and lower (LL) limits of the control, respectively. In addition, a counter was implemented in the system to count the number of points exceeding the determined range of performance.

Error adjustment in the method of temperature measurement

One important factor, responsible for defining the adjustment parameters, N and $m + 1$ of T_{reg}, beyond the graphical observation, is to calculate the root mean square error RMSE between T_{reg} and T_{proc}, given by Eq. (15) where η is the sample size.

$$\text{RMSE} = \sqrt{\frac{1}{\eta}\sum_{i=1}^{\eta}(T_{reg} - T_{proc})^2} \tag{15}$$

Results and discussions

Evaluation of fermentation performance

Table 1 shows the temperatures collected by the acquisition system during fermentation, as described in "Procedures for obtaining the best fermentation performance". It is important to remember that the heating chamber was maintained at $T_{room} = 303.15$ K, and other parameters were defined with their respective units in "Procedures for obtaining the best fermentation performance".

Although, the fermentations 10 and 11 reached the highest temperatures, they presented a shorter duration in comparison with the others, i.e., yeasts of these fermentations were not able to maintain the maximum alcohol yield for a longer duration of time. The common factor among these fermentations is the use of 10 g of yeast, i.e., probably, there was a significant amount of competition between the microorganisms. Excluding the fermentations 9 and 14, this amount of yeast used was not considered to generate

Table 1 Experiments carried out to determine the best fermentations

F_n	M_Y	D_J	$T_{proc,f}$ (max)	$T_{ind,f}$ (max)	$T_{proc,c}$	$T_{ind,c}$	$\Delta T_{proc,f-c}$	$\Delta T_{ind,f-c}$	Δt_f
01	5.4	66.7	305.816	305.857	303.497	303.558	2.319	2.299	9
02	5.4	10.0	303.954	303.967	302.779	302.774	1.175	1.193	4.5
03	5.4	100	306.508	306.519	303.234	303.269	3.274	3.250	13.6
04	5.4	50.0	306.275	306.304	303.174	303.239	3.101	3.065	9
05	3	10.0	303.457	303.474	302.438	302.505	1.019	0.969	4.5
06	3	100	305.503	305.521	302.989	302.945	2.514	2.576	18
07	3	50.0	305.319	305.330	303.301	303.346	2.018	1.984	11.3
08	3	66.7	305.858	305.835	303.534	303.559	2.324	2.276	12.7
09	10	100	308.038	308.014	304.482	304.535	3.556	3.479	13.6
10	10	66.7	308.282	308.270	304.129	304.199	4.153	4.071	8.1
11	10	50.0	307.468	307.478	303.170	303.243	4.298	4.235	7.2
12	1	50.0	304.618	304.604	303.653	303.626	0.965	0.978	11.3
13	1	66.7	304.841	304.854	304.097	304.118	0.744	0.736	20.3
14	10	10.0	304.595	304.588	303.199	303.278	1.396	1.310	6.8
15	1	100	304.898	304.876	303.850	303.944	1.048	0.932	18
16	1	10.0	303.905	303.873	303.108	303.181	0.797	0.692	6.8

the best quality of fermentation in this work. Following the similar criterion, fermentations that presented low temperatures (close to the control), such as 02, 05, 12, 13, 15, and 16 were not considered, because it is indicated that these fermentative processes had an extremely low yield, and there was very little heat released per consumed molecule. In this way, it is observed that diluting the cane juice in water at 10% and/or using 1 g of yeast may not have been an efficient method for fermentation, because it made a small amount of substrate available to the yeast and/or the amount of yeast used was lesser than that demanded by the process.

Thus, the fermentations 01, 03, 04, 06, 07, and 08 presented better performance, because they maintained high temperatures for a longer time, such as fermentation 01, whose graph is shown in Fig. 3.

Conclusively, the best fermentation performances are obtained by combinations containing 3 and 5.4 g of yeast and diluted juice in 50 and 66.7%, and (100%) pure undiluted juice.
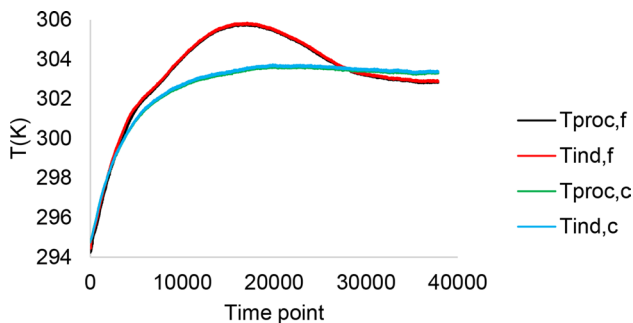
Fig. 3 Temperature vs. time plot corresponding to fermentation 01 containing 5.4 g of yeast in 66.7% diluted juice. The duration of observed process was 9 h (or 20,000 time points, corresponding to the interval of 7000–27,000 points)

Evaluation of the temperature regulation method

The data saved from each of the best fermentations were run in the implemented numerical method system, which, keeps the following parameters fixed: $M = 4.7 \times 10^{-6}$ kg, $C = 3.8 \times 10^2$ J/kg K, $A = 3.14 \times 10^{-2}$ m^2, $\varepsilon = 0$, d$t = 0.001$ s, and $T_0 = 373.5$ K, which refers to the first entry data point of temperature. This is due to the usage of the same thermocouple for each experiment. At each run, τ and RMSE were evaluated, which depends on the variation of N and $m + 1$ of the polynomial and also the inserted h_{proc} (shown in Eq. (3) for τ determination). The input and output values of h_{proc} and τ, respectively, are shown in Table 2 and is applicable to all fermentation processes.

According to the previously conducted work [16], the best fit of the numerical method implies a τ of numerical magnitude equivalent to 10^0 s, i.e., about 1 s, because, it adequately composes the inverse problem, reducing the problems of the expected ill condition, typical in such methods. Despite the different magnitudes of τ, their values relate to 1.03416, because, the weight of the SMLS's polynomial considered in this work is 1. One of the most suitable values of τ is 1 s, and the value of h_{proc}, which should be used as a reference for the adjustment of this coefficient, is 550 W/m² K.

Any study of convection processes usually reduces to a study of procedures, by which its convection coefficient can

Table 2 Relation between inserted h_{proc} and output τ to all fermentations

h_{proc} (W/m² K)	550	5500	55,000	550,000
τ (s)	1.03416	0.103416	0.0103416	0.00103416

be determined. However, convection will often arise as a boundary condition in solution of problems involving conduction, and in such cases, the known values of convection coefficient which are tabulated can be used. In some of the cases, where natural convection occurs in liquids, such as the case of submerged fermentation in this work, these values range from 50 to 1000 W/m² K [8]. Thus, defining h_{proc} as 550 W/m² K is not only due to the proper determination of τ, but also because it composes one of the characteristic values of the convection coefficient, respecting the expected behavior of thermodynamics.

While calculating the RMSE error, it was observed that for low values of N, and high values of $m + 1$ in the polynomial function, the error is low. However, when the polynomial function is calculated with $m + 1 > 10$, a delay is created in signal reconstruction of T_{reg}, because, the calculations corresponding to higher $m + 1$ require more time to be realized. Moreover, observing the graphic behavior, and choosing $N \geqslant 3$, completely uncharacterizes the regularization method, because it amplifies the graph noise and distances itself from T_{proc}, which often presents noises greater than those produced naturally by reconstruction from the inverse
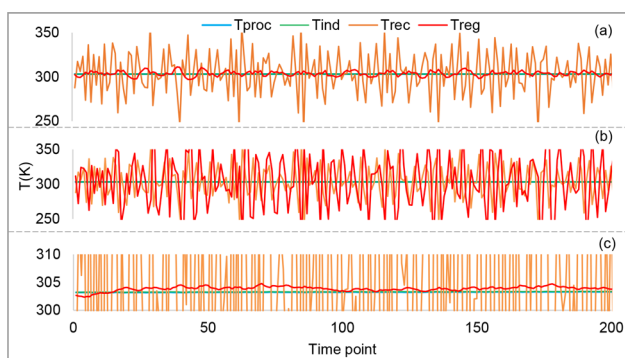

Fig. 4 Temperature adjustment of the fermentation 01 using a polynomial of **a** $N = 1$ and $m + 1 = 8$; **b** $N = 4$ and $m + 1 = 8$; and **c** $N = 1$ and $m + 1 = 30$. In all cases, $h_{proc} = 550$ W/m² K

problem, as represented by T_{rec} [16]. These results are illustrated in Fig. 4b shows an uncharacterized T_{reg}, which clearly presents the amplified noise in relation to T_{rec}, due to the choice of $N = 4$, and for a fixed $m + 1 = 8$. In Fig. 4c, we can see that due to the choice of $m + 1 = 30$, in the adjustment polynomial T_{reg} lags behind T_{rec} by a large amount. This requires a large number of points for the polynomial function, to calculate each reconstruction point, even if N is kept as 1. Both Fig. 4b, c are in contrast with the good regularization observed in Fig. 4a, which uses $N = 1$ and $m + 1 = 8$, as parameters of the method polynomial function. Thus, it should be noted that to have an acceptable temperature setting, a polynomial should be chosen with $N = 1$ or 2 and $2 \leq (m + 1) \leq 10$.
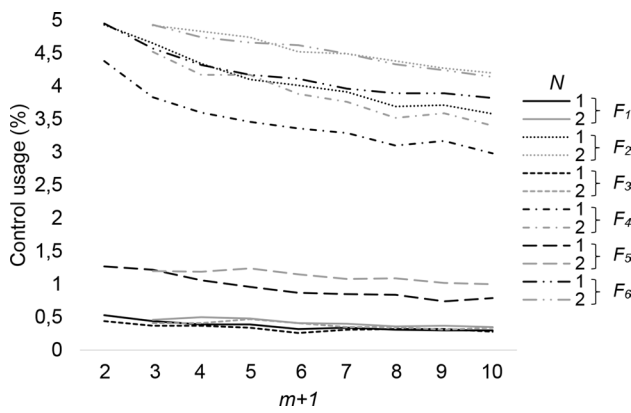
Evaluation of the best performance fermentations

The best obtained fermentations maintained their performance as discussed in "Evaluation of fermentation performance" of this paper. However, in this item, two pairs of thermocouples were used in these fermentations to read the temperature from the same fermentation. The first pair is given as $T_{procA,f}$ and $T_{indA,f}$, and second, $T_{procB,f}$ and $T_{indB,f}$. It can be observed that both the $T_{proc,f}$ s reach a maximum satisfactory temperature and, in general, is greater than its respective $T_{ind,f}$. This is probably due to the encapsulation in $T_{ind,f}$, which causes delays in the response time. Furthermore, most data on fermentation show that, both $T_{ind,f}$ end up accumulating heat in these capsules and take longer to lower the temperature in relation to the encapsulated thermocouples and, therefore, they are often higher than the $T_{proc,f}$.

These series of data on temperature, when run into the implementation of the program according to the data defined in "Evaluation of the temperature regulation method", generate two temperature graphs, the first corresponding to the pairs of thermocouples A and B, and both similar to that of Fig. 5a, when duly adjusted. From this step onwards, it is possible to generate a common convection coefficient of the
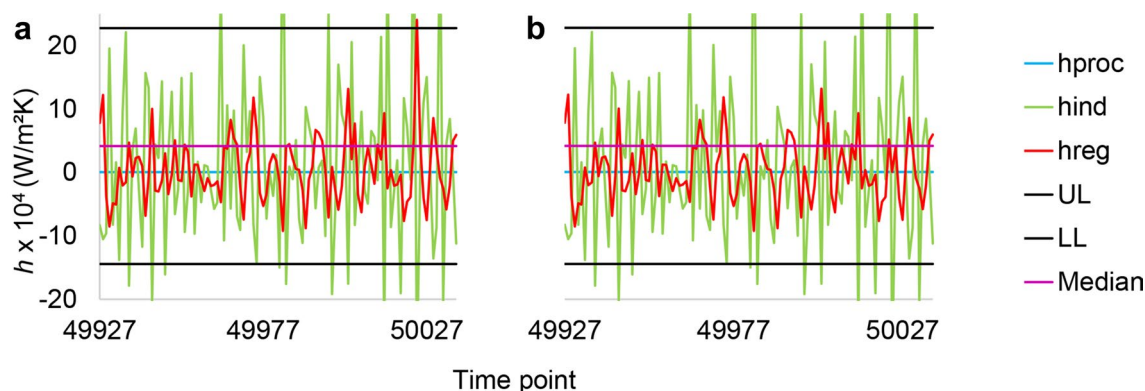
Fig. 5 Monitoring of the convection coefficient (**a**) and control of h_{reg} (**b**)

Fig. 6 Use of the control for every improved performance of fermentation F_n, considering $N = 1$ or 2 and $m + 1$ varying from 2 to 10

process and apply the regularization method necessary to determine its range of performance.

Evaluation of the regularization method and determination of h

The execution of each of the best fermentation processes comprises of varying N between 1 and 2, in combination of $m + 1$ within 2 and 10 with an interval of 1, other values of the input variables were fixed in accordance with "Evaluation of the temperature regulation method". The data from h_{reg}, generated while monitoring, were saved, and subsequently, run in the threshold system, which were separately implemented according to Eqs. (13) and (14). Each value of λ and their medians, obtained by this system, served as the basis for calculating the averages of these parameters, which were used to determine the range of common convection coefficient generated at each adjustment.

Each one of the high-performance fermentations was again run with the previously described fixed input data, including the average values of λ and median, corresponding to the chosen N and $m + 1$ for adjustment. Hence, the control graph counter was applied when the points were above or below the UL and LL, respectively. Figure 5a shows the monitoring of convection coefficient, performed by the numerical method, along with the delimitation of its action range by UL and LL. Figure 5b depicts the control of the convection coefficient obtained by the same method, but the difference being, that the points outside the operating range received the h_{proc} value, and these points were added to the control usage.

The control usage is given in percentage corresponding to each process, represented in Fig. 6, by varying and N and $m + 1$.

It is observed that there is a tendency of the control to be used lesser when $m + 1$ increases, as well as when $N = 1$ as compared to, when $N = 2$. The behavior of the adjustment convection coefficient graph, in which the mismatch adjustment and amplified reconstruction noise are neglected, was also analyzed. Table 3 shows the best N and $m + 1$ necessary for adjusting the convection coefficient. It is important to highlight, that, the control was used in less than 5% of all observed cases, and often close to 0%. This means that, while monitoring, the refinement in adjustment is sufficient to maintain the results within the range of the convection coefficient.

Corresponding to these parameters of the regularization method, the performance range of the convection coefficient presents λ and the median average values, as shown in Tables 4 and 5.

Table 3 Combinations of N and $m + 1$ for attaining good fit of convection coefficient

$m + 1$	4	5	6	7	8	9	10
N	1	1	1 e 2	1 e 2	1 e 2	1 e 2	2

Table 4 Average values of λ varying as a function of adjustment parameters

$N/m + 1$	4	5	6	7	8	9	10
1	148,475.0	104.817.2	79,144.03	62,726.17	51,685.97	43,410.13	37,290.92
2	519,328.7	368,639.5	282,051.3	225,371.8	185,951.5	156,658.3	134,902.5

Table 5 Average median values varying as a function of adjustment parameters

$N/m + 1$	4	5	6	7	8	9	10
1	33,240.88	23,465.72	17,717.58	14,041.63	11,571.09	9718.238	8348.108
2	116,269.7	82,531.62	63,143.84	50,454.13	41,629.87	35,071.56	30,200.22

Conclusions

This work provided artifices that collaborated with the achievement of a better performance of fermentations, along with the definition of the numerical method parameters necessary to obtain proper bioprocess monitoring and control. This is accomplished by the definition of the reconstructed temperature, and the regularized convection coefficient common to the fermentation medium.

It was verified, that to obtain the best results of fermentations, in addition to pure juice, a combination of 3 or 5.4 g yeast in 50%, 66.7% of water-diluted juice should be used. It was observed that, besides lasting longer, such fermentations may be reached at maximum temperatures of about 306 K, when compared to the other previously tested fermentation processes.

By analyzing the adjustment applied to the temperature signals, obtained from the best performance fermentations, it was observed, that to have an acceptable adjustment, using the numerical method, a polynomial of $N = 1$ or 2 and $2 \leq (m + 1) \leq 10$ should be chosen. Furthermore, the h_{proc} input data equals to 550 W/m^2 K, which is consistent with values reported in literature [8]. The same conditions are applicable when two pairs of thermocouples are considered for the same fermentation process.

Determining the convection coefficient of the fermentative process has other aspects along with the observation of the application of numerical method, which provides a restricted performance range for its proper monitoring. It is also possible to apply a statistical control to the points outside this range, which, in turn, occurs in less than 5% of the cases, indicating, that the regularization method itself can restrict h_{reg} within the range. Thus, defining this performance range allows the method to be further refined with its relevant parameters. Finally, it can be said that there is availability of the proposed mathematical model to be applied for pilot and industrial scale without compromising process and method, since once temperature is acquired during the process, the regularization principle is the same. Also, considering the numerical technique in question, scaling-up would imply, at first, in use of more robust thermocouple, which would, consequently, amplify noise and reading delays of temperature, but still be able to be readjusted by the method [16].

References

1. Balat M, Balat H, Oz C (2008) Progress in bioethanol processing. Prog Energy Combust 34:551–573
2. Bayer FM, Kozakevicius AJ (2010) SPC-threshold: Uma proposta de limiarização para filtragem adaptativa de sinais. TEMA Tend Mat Apl Comput 11:121–132
3. Bazán FSV, Borges LS (2004) In: Barcelos CAZ, Andrade EXL, Boaventura M (eds) Notas em Matemática Aplicada. SBMAC, São Carlos
4. British Petroleum Global (2017) BP statistical review of World energy. http://www.bp.com/content/dam/bp/pdf/energy-economics/statistical-review-2016/bp-statistical-review-of-world-energy-2016-full-report.pdf. Accessed 3 Feb 2017
5. Colaço MJ, Orlande HRB (2004) Inverse natural convection problem of simultaneous estimation of two boundary heat fluxes in irregular cavities. Int J Heat Mass Transf 47:1201–1215
6. Corazza ML, Rodrigues DG, Nozaki J (2001) Preparation and characterization of orange wine. Quím Nova 15:449–452
7. Donoho DL, Johnstone IM (1994) Ideal spatial adaptation by wavelet shrinkage. Biometrika 81:425–455
8. Incropera FP, Dewit DP, Bergman DL, Lavine AS (2008) In: Queiroz EM, Pessoa FLP (eds) Fundamentos de transferência de calor e de massa, 6th edn. LTC, Rio de Janeiro
9. Kobayashi M, Nagahisa K, Shimizu H, Shiova S (2006) Simultaneous control of apparent extract and volatile compounds concentrations in low-malt beer fermentation. Appl Microbiol Biotechnol 73:549–558
10. Kozakevicius AJ, Bayer FM (2014) Signal denoising via wavelet thresholding. Cien Nat 36:37–51
11. Kumar S, Dheeran P, Singh SP, Mishra IM, Adhikari DK (2013) Cooling system economy in ethanol production using thermotolerant yeast Kluyveromyces, sp. IIPE453. J Microbiol Res 1:39–44
12. Lima UA, Basso LC, Amorim HV (2001) In: Lima UA, Aquarone E, Borzani W, Schmidell W (eds) Biotecnologia industrial. Edgard Blücher, São Paulo
13. Liu CS, Kuo CL, Jhao WS (2016) The multiple-scale polynomial Trefftz method for solving inverse heat conduction problems. Int J Heat Mass Transf 95:936–943
14. Mirsephai A, Mohammadzaheri M, Chen L, O'Neill B (2012) An artificial intelligence approach to inverse heat transfer modeling of an irradiative dryer. Int Commun Heat Mass Transf 41:19–27
15. Mohanraj K, Nair NV (2014) Biomass potential of novel interspecific hybrids involving improved clones of *Saccharum*. Ind Crop Prod 53:128–132
16. Oliveira J, Santos JN, Seleghim P Jr (2006) Inverse measurement method for detecting bubbles in a fluidized bed reactor—toward the development of an intelligent temperature sensor. Powder Technol 169:123–135
17. Paz PM, Oliveira J (2013) Use of a numerical technique for monitoring of convection coefficient in industrial processes. In: 22nd international congress of mechanical engineering. http://www.abcm.org.br/anais/cobem/2013/PDF/322.pdf Accessed 20 Jan 2017
18. Peixoto CRM, Rosa GR, Silva CN, Santos BT, Engelmann L (2012) Miniprojeto para ensino de química geral experimental baseado na fermentação do caldo de cana de açúcar. Quím Nova 35:1686–1691
19. Salvadó Z, Arroyo-López FN, Barrio E, Querol A, Guillamón JM (2011) Quantifying the individual effects of ethanol and temperature on the fitness advantage of *Saccharomyces cerevisiae*. Food Microbiol 28:1155–1161
20. Tikhonov AN, Arsenin VY (1977) Solutions of ill-posed problems. Wiley, New York